INTERNATIONAL JOURNAL OF HYDROGEN ENERGY 41 (2016) 8606–8615

Available online at www.sciencedirect.com

ScienceDirect

journal homepage: www.elsevier.com/locate/he

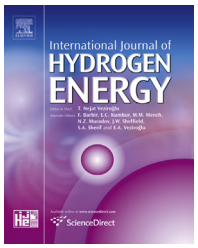

The role of initial tank temperature on refuelling of on-board hydrogen tanks

N. de Miguel[*], *B. Acosta*, *D. Baraldi*, *R. Melideo*, *R. Ortiz Cebolla*, *P. Moretto*

Institute for Energy and Transport, Joint Research Centre, European Commission, Westerduinweg 3, 1755ZG Petten, The Netherlands

ARTICLE INFO

Article history:
Received 20 November 2015
Received in revised form
23 March 2016
Accepted 23 March 2016
Available online 22 April 2016

Keywords:
Compressed hydrogen storage
Hydrogen refuelling
Initial tank temperature
Hydrogen safety
Computational fluid dynamics

ABSTRACT

The influence of the initial tank temperature on the evolution of the internal gas temperature during the refuelling of on-board hydrogen tanks is investigated in this paper. Two different types of tanks, four different fuel delivery temperatures (from ambient temperature refuelling to a pre-cooled hydrogen at −40 °C), several filling rates and initial pressures are considered. It has been found that the final gas temperature increases linearly with the increase of the initial tank temperature while the temperature increase (ΔT) and the final state of charge (SOC) decrease linearly with increasing the initial temperature. This dependency has been found to be larger on type III than on type IV tank and larger the larger the initial pressure. Additionally CFD simulations are performed to better understand the role of the relevant phenomena on the gas temperature histories e.g. gas compression, gas mixing, and heat transfer. By comparing the results of calculations with adiabatic and diathermal tank walls, the effect of the initial gas temperature has been separated from the effect of the initial wall temperature on the process.

Introduction

The need for reducing greenhouse gas emissions and the limitation of available non-renewable energy resources make compulsory the use of alternative fuels. Hydrogen, with higher energy content per unit mass than any known fuel can play an important role as a future energy carrier. In the transportation sector, fuel cell vehicles (FCV) powered by hydrogen could replace the traditional oil-derived fuel cars. However, there are still several barriers including hydrogen production, distribution, refuelling and the vehicle design itself which impede its massive diffusion in the automotive sector [1]. Regarding hydrogen storage, specific on-board storage technologies are necessary to match the typical energy densities of the traditional liquid fuels (gasoline or diesel). Currently, the most commonly adopted storage solution by car manufacturers is compressed hydrogen storage [2]. Gaseous hydrogen is stored on-board the vehicle in fully wrapped carbon fibre reinforced tanks. In order to reach high hydrogen densities, the gas is stored at high pressures. Hydrogen tanks with a nominal working pressure (NWP) of either 35 or 70 MPa are already in the market. Two types of liners are typically used in these tanks: metal in type III tanks and a polymer liner in type IV tanks [3].

The refuelling of on-board hydrogen tanks has to be performed in a reasonable amount of time. According to the European Fuel Cells and Hydrogen Joint Undertaking (FCH-JU),

* *Corresponding author*. Tel.: +31 224 565395; fax: +31 224 565645.
E-mail address: nerea.de-miguel-echevarria@ec.europa.eu (N. de Miguel).

http://dx.doi.org/10.1016/j.ijhydene.2016.03.158

one of the technological challenges for the successful implementation of FCVs is to reduce the refuelling times to 3–4 min for passenger cars [4]. This is in line with the technical system targets for 2020 of the United States Department of Energy (DoE) for light duty fuel cell vehicles which set to 3.3 min the fuelling time of a 5 kg hydrogen on-board storage system [5]. During the refuelling, the compression work leads to a warming of the gas inside the tank. The final temperature within the tank can have an impact on the safety (tanks are designed to work between −40 °C and 85 °C [6–8]) but also on the level of filling of the tank; for the same pressure, the higher the temperature the lower the gas density. The level of filling is characterized by the State of Charge (SOC) which represents the ratio (in percentage) between the density of hydrogen inside the tank and its density at the NWP and 15 °C (40.2 kg/m^3 at 70 MPa NWP) [2]. To be able to refuel a vehicle in a practical amount of time without reaching the temperature limits and with a reasonable level of filling, the Society of Automotive Engineers (SAE) has established the SAE J2601, a standard for hydrogen fuelling protocols [9]. The SAE J2601 proposes refuelings based on a look-up table approach. The process limits (including the target pressure and pressurization rate) are determined by aspects such as ambient temperature, fuel delivery temperature, the size and the initial pressure of the compressed hydrogen storage system (CHSS). The CHSS consists of all the components that form the primary high pressure boundary for containment of compressed hydrogen including one or more than one tank depending on the amount that needs to be stored and the particular vehicle design [6].

It is known that the parameters of the CHSS to be filled (namely size, materials and initial temperature and pressure) together with the filling conditions (such as filling rate, final pressure and gas delivery temperature) determine the temperatures reached inside the tanks at the end of the refuelling [10–12]. The initial temperature of a tank when refuelled is normally assumed to be the same to the outside temperature; however, it could be warmer or colder than the ambient. The tank can be for instance heated up to 25 °C higher than the surroundings during parking or driving if being heated by the sun's rays [2]. On the other hand, under average driving conditions, when continuously emptying a full tank down to 20% SOC and due to the cooling of the gas during the expansion, the on-board tanks of the car could arrive to the refuelling station at a temperature at least 20 °C lower than the ambient temperature [13]. These situations could result in refuelings where the temperature inside the tank is higher or lower than the expected one leading to overheating or overfilling of the tanks. To avoid this, hot soak and cold soak zones are considered in the 2014 version of the SAE J2601 [9].

The initial temperature of the tank (assuming the tank in thermal equilibrium with the ambient temperature at the beginning of refuelling), as originally found by Maus [10] and later confirmed by other authors [14,15], has a linear effect on the maximum gas temperature during refuelling. Maus found that when refuelling a 70 MPa type III tank, an increase of 1 °C in the initial temperature results in a growth of 0.8 °C in the maximum temperature. Zhao et al. [14] on the other hand found that when refuelling a 35 MPa type III tank, an increase of 1 °C in the initial temperature results in a 0.3 °C increase of the maximum temperature. The aim of the work presented in this article is to further investigate the influence of the initial tank temperature on the evolution of the gas temperature during hydrogen refuelling. Several refuelling experiments have been carried out in both type IV and type III tanks at several initial tank temperatures. In particular, we have investigated the case of refuelling with different hydrogen pre-cooling levels (different fuel delivery temperatures) for relatively high initial tank temperatures. To assist the interpretation of the experimental results and to perform experiments at conditions not achievable at the experimental facility, numerical simulations of hydrogen refuelling of one of the tested tanks have been also carried out with a Computational Fluid Dynamics (CFD) model.

Experimental

GasTeF facility

The Gas Tank Testing Facility, GasTeF, is a laboratory of the European Commission's Joint Research Centre which aim is the testing of compressed hydrogen tanks [16]. The tanks are placed inside a 380 L volume closed sleeve which at the same time is enclosed in a safety vessel. The sleeve is maintained under a continuous flow of nitrogen. The sleeve temperature can be modified from ambient temperature up to 85 °C by means of a resistance heating that surrounds it over its entire

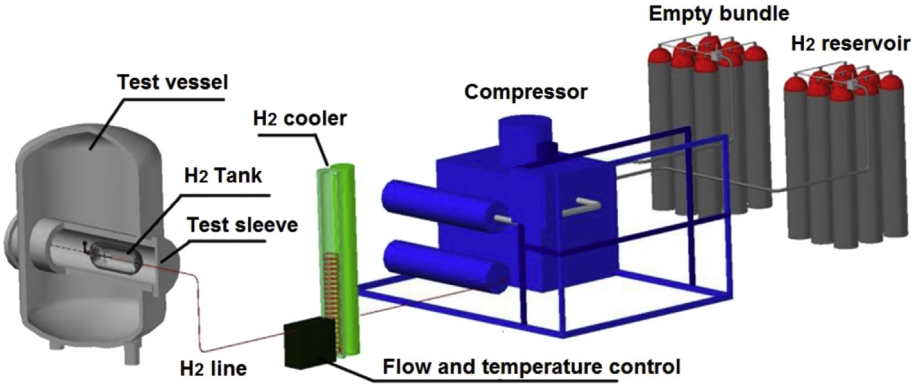

Fig. 1 – Scheme of the GasTeF facility.

Table 1 – Characteristics of the tested type IV and type III tanks.

	Type IV	Type III
Materials		
Liner	HDPE	AA
End bosses	SS	AA
Composite shell	G&CFRE	CFRE
Vessel Mass (Kg)	32.9	41.5
Storage Volume (L)		
(at 70 MPa)	29	40
H_2 capacity (Kg)		
(fill density of 40.2 kg/m^3)	1.16	1.60
Unpressurized dimensions (mm)		
External length	827	920
External diameter	279	329
Internal diameter	230	290

HDPE: High density polyethylene, CFRE: Carbon fibre reinforced Epoxy, G&CFRE: Glass and carbon fibre reinforced Epoxy, AA: Aluminium alloy, SS: Stainless steel.

surface. The delivered hydrogen can be pre-cooled (before entering the tank) by a gas chiller (a liquid nitrogen heat exchanger) placed between the test vessel and the compressor. In Fig. 1, a scheme of the GasTeF facility is shown. For safety reasons, the whole GasTeF but the storage area is enclosed inside a half-buried concrete bunker which is freed from oxygen while the tests are running. Tests are controlled and monitored remotely from a control room.

As already described in a previous work [17] the filling of the tanks is performed in two stages. The first consists in a pressure equilibration between an external hydrogen reservoir and the tank under test. When the pressure of the tank is equilibrated with the one in the gas reservoir, the compressor fills the tank to the required final pressure at the required speed. The combination of the two stages results generally in a non-linear pressure rise profile. More importantly, also the mass flow rate is not constant, a situation very similar to the real-cases in refuelling stations. Therefore, the value of the mass flow rate given in this paper, called Average Mass Ramp Rate (AMRR), represents an average value calculated considering the total time required for reaching the final mass. For the mass calculation, we use the Redlich-Kwong equation of state for real gases which accurately predicts hydrogen properties in a wide range of temperatures and pressures [18].

Characteristics and instrumentation of the tanks

Two different 70 MPa NWP on-board hydrogen storage tanks, a type IV of 29 L capacity and a type III of 40 L, have been used in this study. In Table 1, the characteristics of the tanks are given. As depicted in Fig. 2, each tank has been instrumented with several thermocouples (TC) and several resistance temperature detectors (RTD). The TCs (labelled from 1 to 8) measure the temperature of the gas at different positions. The RTDs (labelled T_{Front}, T_{Rear}, T_{Top} and T_{Bottom}) are placed on the outside of the tank to measure the temperature of the bosses and of the tanks walls. The gas delivery temperature, T_{delgas}, was measured with a sensor placed inside the hydrogen line just 10 cm before entering the tank. The pressure has been measured using a pressure transducer placed at the rear of the tanks. The temperature and pressure at the tank inlet line have been also controlled. The details of all the instrumentation placed in the tanks can be found in Refs. [16], [17]. In all cases and to get homogeneous temperatures during the filling, a 3 mm diameter hydrogen dispenser has been used [19].

The CFD model

In order to understand better the occurring phenomena, a validated Computational Fluid Dynamics (CFD) model developed at JRC [20,21], has been used. The model is based on commercial CFD software ANSYS CFX V14.0 [22]. The numerical time scheme is based on a Second Order Backward Euler scheme. The CFX high resolution scheme has been selected for the advection terms. A residual convergence criterion for RMS (root mean square) mass-momentum-energy equations of 10^{-4} has been applied. At high pressures, the ideal gas law is not capable of accurately describing the gas pressure and temperature behaviour. Therefore a real gas equation of state has been selected (Redlich and Kwong [18]). A modified k-ε model [23] was applied as turbulence model in order to reduce the jets spreading rate over-prediction of the standard model [24–27]. It is assumed that the gas and the tank material are initially at the same temperature.

The conjugate heat transfer model (CHT) has been used in order to describe the heat transfer through solid materials coupled with the changing temperature in the fluid. The heat transfer coefficient on the outer surface of the tank is assumed to be 6 W/K.m^2. Non-slip boundary conditions are applied to

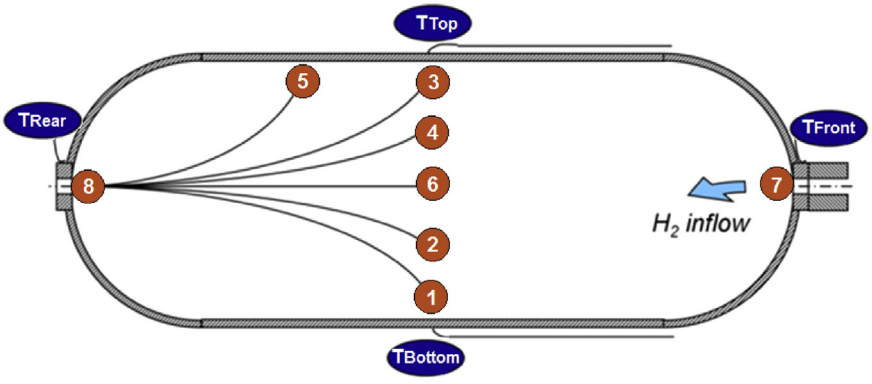

Fig. 2 – Arrangement of the temperature measurement instrumentation in the tested tanks.

all tank walls. The tank material properties have been selected according to Monde [11].

The computational model has been generated with five subdomains: the gas subdomain (i.e. the tank interior filled by hydrogen), the internal liner, the external composite carbon fibre wrap (CFRP) and the two bosses at the tank ends.

Refuelling experiments and simulations

Experiments at GasTeF

Several fillings, representative of on-board hydrogen tanks refuelling, have been performed with the described type III and type IV tanks. The fillings have been done at different initial temperatures in the range between 20 °C and 50 °C. Fillings started when both hydrogen within the tank and tank walls were in thermal equilibrium with the surrounding sleeve and when the difference between gas temperature measured by the TCs and tank temperature measured by RTDs was $\leq$ 2 °C. In Table 2, the conditions of the performed tests are summarized. The pressure range was the same in all cases; the tanks were filled from 2 to 77 MPa. In a first set of experiments, both tanks were filled at a comparable AMRR (of 3.3–3.7 g/s) resulting in different fill times depending on the tank volume. The hydrogen was delivered without being pre-cooled (at 25 °C). In a second set of experiments, and to study the effect of the fuel delivery temperature, the filling time was fixed at 200 s, with a deviation between fillings of ±10 s and the fuel delivery temperature was varied from −40 °C to 25 °C, with a deviation of ±2 °C on each group of experiments. In order to study the effect of the initial pressure, a series of fillings starting at an initial pressure of 10 MPa were performed on the type IV tank at 5 g/s and at two different fuel delivery temperatures; 2 °C and −40 °C.

The following parameters have been calculated for the mentioned cycles:

a) The averaged gas temperature, T_{Av}, defined as the average of 5 temperatures measured from top to bottom in the tanks, TC3, TC4, TC6, TC2 and TC1 and which have been found to follow the same temperature profile during the filling [12].
b) The gas temperature increase due to the refuelling, ΔT_{Av}, calculated as the difference between the final and initial gas averaged temperatures: $\Delta T_{Av} = T_{Av}$ (end filling) − T_{Av} (start filling) = $T_{FAv} - T_{0Av}$.
c) The averaged gas delivery temperature, $T_{delgasAv}$, calculated as the time-averaged gas temperature with values measured along the whole filling period.

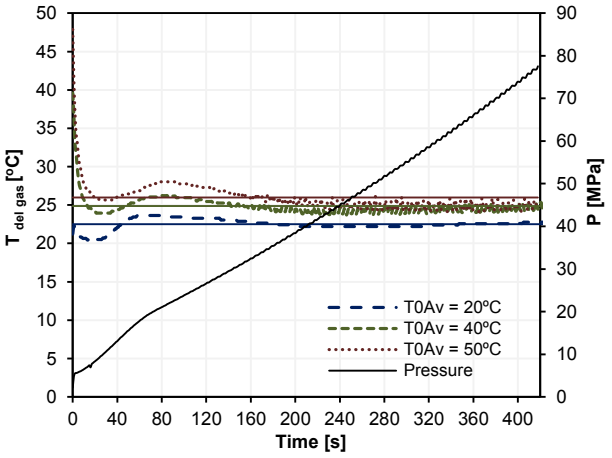

Fig. 3 – Evolution of the delivery gas temperature (without pre-cooling) during the filling of type III tank with an AMRR of 3.3 g/s and for initial tank temperatures of 20 °C, 40 °C and 50 °C.

In Fig. 3 an example of the evolution of the gas delivery temperature during the filling of a type III tank without pre-cooling and at three different initial tank temperatures (of 20 °C, 40 °C and 50 °C) is given. Due to the warming of the sleeve, the delivery pipe inside the sleeve remained warm. This resulted in a higher temperature of the gas entering the tank the higher the initial temperature. This can be clearly observed in the averaged gas delivery temperatures shown with continuous lines in Fig. 3. In the experiments, the tank pressure change inside the vessel follows closely the pressure behaviour of the one at the tank inlet. The pressure profiles are depicted in Figs. 3–5. Those pressure profiles have been used as inputs for the CFD simulations.

Refuelling simulations at JRC

Fast fillings of type IV tank (see Table 2) have been simulated using the CFD model developed at JRC. Some initial conditions (below the ambient temperature) that could not be reproduced in the experimental facility have been considered. Three different initial temperatures were chosen; −20 °C, 0 °C and 30 °C. At the tank inlet, the gas delivery temperature was kept constant at 0 °C in all calculations while the gas pressure increased from 2 MPa to 77 MPa in 200 s. Two types of boundary conditions have been assumed; "diathermal walls conditions" and "adiabatic conditions". In the first series of simulations, the heat transfer between the tank walls and the

Table 2 – Experimental and simulation conditions of the refuelling experiments performed on type IV and type III tanks.

	Type IV			Type III		Type IV CFD	
Initial Pressure (MPa)	2	2	10	2	2	2	10
Final Pressure (MPa)	77	77	77	77	77	77	
Filling time (s)	270	200	175	420	220	200	175
Av. filling rate (AMRR) (g/s)	3.7	5.0	5.0	3.3	6.5	5.0	
Av. gas delivery temperature (°C)	25	−40; −17; 2; 20	2; −40	25	−40; −17; 2; 25	0	
Initial temperature (°C)		20–50			20–50	−20; 0; 30	

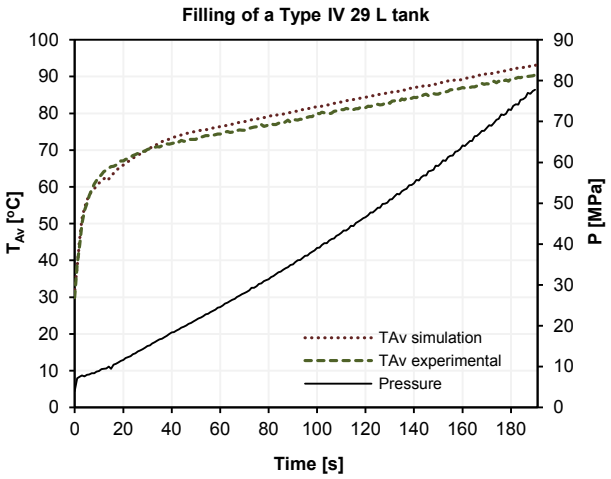

Fig. 4 – Comparison of the experimental and simulated (for diathermal walls) average temperature profiles for fillings of type IV tank starting from equilibrium at 30 °C and with the delivery gas at 0 °C.

gas and between the walls and the surrounding environment has been taken into account in the model. In the second series of simulations, the gas is considered thermally isolated from the tank walls.

Validation of the CFD model

In Fig. 4, the gas average temperature profiles obtained experimentally (in the GasTeF facility) and the equivalent obtained through a simulation (considering diathermal walls) are shown. As it can be observed in Fig. 4, the temperature profile calculated with the CFD model follows very closely the experimental curve (with less than 3 °C difference with the experimentally obtained temperature at the end of the filling) giving confidence about the model.

The increase of the gas temperature inside the tank is caused by the following mechanisms: the gas compression, the conversion of kinetic energy into internal energy, and the Joule-Thomson effect. The gas compression and the energy conversion are automatically taken into account into the CFD model by the fluid governing equations for the conservation of the mass, momentum and energy. The Joule-Thomson coefficient, for a pressure range between 2 MPa and 78 MPa has a value which goes from −0.264 to −0.505 °C/MPa at 0 °C [26]. That would mean a potential temperature increase from 2.64 °C to 5.05 °C for a pressure difference of 10 MPa. The Joule-Thomson effect is negligible for the experimental configuration that is under consideration in this paper. The pressure and temperature of the incoming gas are measured in the experiment in a point along the pipe that is located close to the inlet. After the measurement point, there are not any valves or devices that can cause a significant change in pressure. Moreover, the pressure drop that the gas undergoes when it enters into the tank is limited because the gas pressure in the tank follows closely the behaviour of the pressure of the incoming gas. In the selected pressure profile for the incoming gas in the simulations (with a delivery gas temperature of 0 °C and 2 MPa initial pressure in the tank), the difference between the pressure at the inlet and the pressure in the tank reaches for a fraction of a second a maximum of about 20 bars within the initial 3 s of the filling and then it drops quickly below 5 bars after 9 s, and below 1 bar after 60 s. That means a maximum temperature increase of less than 0.6 °C at the beginning of the filling and of about 0.05 °C at the end of the filling due to the Joule-Thomson effect. Since the total temperature increase is in the order of several tens of degrees, the contribution of the Joule-Thomson effect is negligible for the selected configurations.

Results and discussion

Influence of the type of tank

In Fig. 5, the average gas temperature profiles observed during the first set of refuelling experiments in type IV and type III tanks at three different initial temperatures (20 °C, 40 °C and 50 °C) are shown. The filling times of each tank were adjusted in order to have fillings with similar AMRR. As it can be

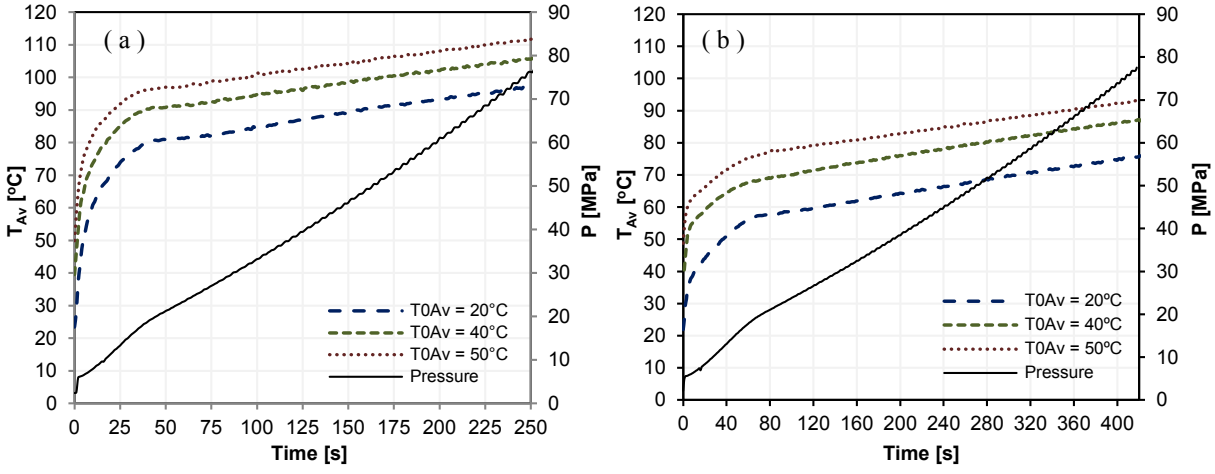

Fig. 5 – Tank averaged gas temperature profiles of fillings of a Type IV (a) and Type III (b) tanks with a delivery gas temperature of 25 °C and for initial tank temperatures of 20 °C, 40 °C and 50 °C.

observed in the figure, the temperature evolution follows the same trend in both tanks. A fast temperature increase occurs in the first seconds of the filling associated to a bigger ratio between the pressure at the inlet line and the pressure inside the tank at the beginning of the filling which results in a bigger mass flow entering the tank [17]. Afterwards, the temperature rises linearly until the end of the filling. As the thermal diffusivity of the aluminium liner is much higher than that of the plastic liner, the heat transfer in type III tank is larger than that in type IV [11]. Consequently, lower final gas temperatures are reached in the type III tank.

In Fig. 6, the average gas temperatures reached at the end of the filling (T_{FAv}) and the temperature increase of the gas (ΔT_{Av}) for the fillings on the type IV and the type III tanks with comparable AMRR and constant gas delivery temperature have been represented against the initial temperature (T_{0Av}). With both tank types, the temperature of the gas reached at the end of the filling, T_{FAv}, has been found to increase linearly with the initial temperature. However, and as it was already observed in our previous work [27], the temperature rise, ΔT_{Av}, decreases with the initial temperature. It can be seen that the slope of the 2 curves, T_{FAv} and ΔT_{Av}, in Fig. 6 are linked to each other, if the following equations are considered (assuming constants A, B, C and D as positive numbers):

$$T_{FAv} = AT_{0Av} + B \quad (1)$$

$$\Delta T_{Av} = T_{FAv} - T_{0Av} = -CT_{0Av} + D \quad (2)$$

From the above expressions, it stems out that:

$$D = B$$

$$|A| + |C| = 1$$

The sum of the absolute values of the slopes must be 1. Therefore a larger slope for T_{FAv} must correspond to a smaller slope for ΔT_{Av}. Moreover, since A is smaller than 1, an increase of initial temperature will generate an increase of the final temperature that is smaller than the increase of initial temperature itself.

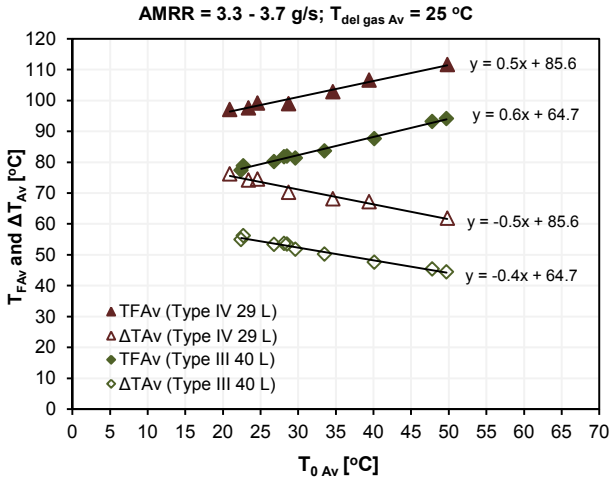

Fig. 6 – Gas temperatures reached at the end of the filling (TFAv) and the temperature increase of the gas (ΔTAv) versus the initial temperature for equivalent fillings of a Type IV and a Type III tank.

Influence of the gas delivery temperature

In Fig. 7, the average gas temperatures reached at the end of the filling (T_{FAv}) of type IV tank (a) and type III tank (b) have been represented against the initial temperature (T_{0Av}). In this set of fillings, the filling time was kept almost constant in both tanks (200–220 s). However, due to the higher internal volume of the type III tank, to reach the same pressure in the same time, the AMRR was higher in type III than in type IV tank. Four different gas delivery temperatures (from no-cooling to −40 °C cooling) were used on each tank.

As observed before, for comparable delivery temperatures, lower final temperatures are reached on type III than on type IV tank, even if the filling rate is larger in the type III than in type IV tank. In both cases, the higher the fuel delivery temperature, the higher are the temperatures reached at the end of the filling. Nevertheless, in all cases the T_{FAv} increases linearly with the increase of the initial temperature, T_{0Av}, and with the same slope regardless the delivery temperature. The slope has been found to be higher in the type III than in the type IV tank. An increase of 1 °C in the initial temperature resulted in an increase of 0.4 °C for the polyethylene liner tank while in an increase of 0.6 °C for the aluminium liner tank. These values are below the 0.8 °C increase (for each 1 °C increase of initial temperature) found by Maus [10] for a 70 MPa type III hydrogen storage system (composed of two tanks with a total volume of 72 L) but above the 0.3 °C increase found by Zhao for a 35 MPa and 150 L type III tank [14].

Influence of the initial tank pressure

In Fig. 8, the average gas temperatures reached at the end of the filling (T_{FAv}) for equivalent fillings of type IV tank starting from 2 MPa to 10 MPa and for initial temperature going from 20 °C to 50 °C have been compared. The tank was filled with hydrogen at 2 °C and at −40 °C. As it can be observed in Fig. 8, when the tank is filled with hydrogen at 2 °C, the previously observed effect of lower temperature reached at the end of the filling with higher initial pressure [14,28], is confirmed. However, it seems that the effect is reduced when the gas is introduced colder. At −40 °C, and for the range of initial tank temperatures studied (20 °C–50 °C), similar gas temperatures have been reached at the end of the filling regardless the initial tank pressure. When the tank is emptier (2 MPa initial pressure), higher mass of colder gas introduced in the tank which might compensate the higher heat of compression introduced in the system when starting at lower pressure. This could be considered as an advantage of using −40 °C precooling in a hydrogen refuelling station. On the other hand, at both hydrogen delivery temperatures, the higher the initial pressure (and higher the mass of gas initially inside the tank) the larger are the slopes of T_{FAv} with T_{0Av}.

Influence of the initial temperature on the SOC

Limiting the maximum gas temperature reached inside the tank at the end of the refuelling is important not only to

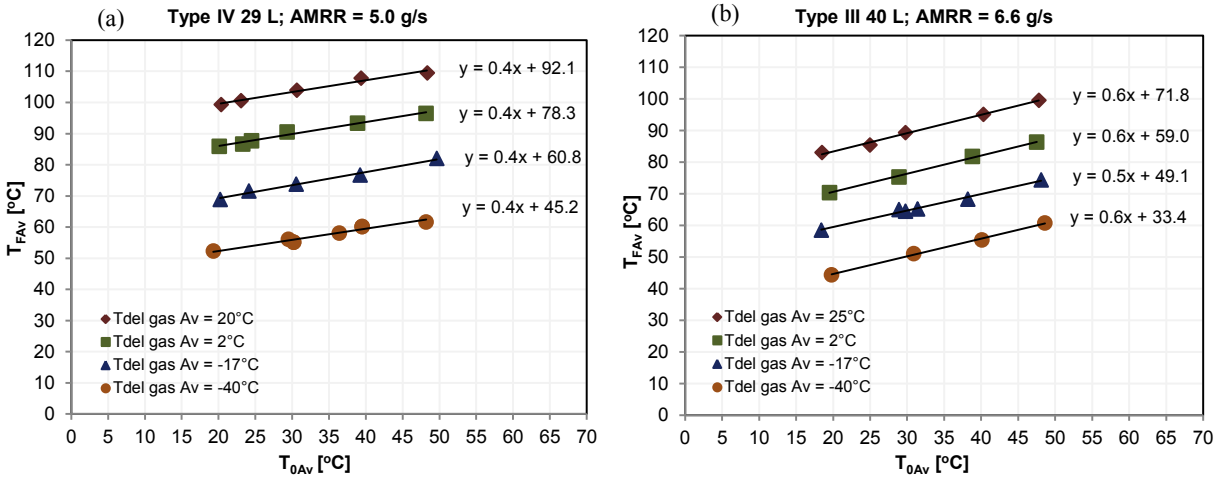

Fig. 7 – The gas temperatures reached at the end of the filling (TFAv) versus the initial temperature for fillings of Type IV (a) and Type III (b) tanks with constant filling rate and for several delivery gas temperatures.

preserve the mechanical properties of the tank materials but also for the final state of charge of the tank [29]. In Table 3, the temperatures reached at the end of the filling, T_{FAv}, and the calculated SOCs in the different tests (for different tanks, different AMRR and different $T_{delgasAv}$) at the two most extreme initial temperatures (20 °C and 50 °C) have been summarized.

As it can be observed in Table 3, the increase of the initial temperature from 20 °C to 50 °C has only an effect of 2%–4% absolute decrease on the final SOC. In general, the goal of the SAE J2601 refuelling protocols is to provide a high density fuelling (SOC > 95%) as fast as possible while staying within the process limits [9]. This was obtained in all the refuelling experiments performed at −40 °C and in few experiments at −17 °C (on a type III tank and at a low initial temperature). For the other conditions, slower refuelings would be necessary to reach such high densities inside the tank.

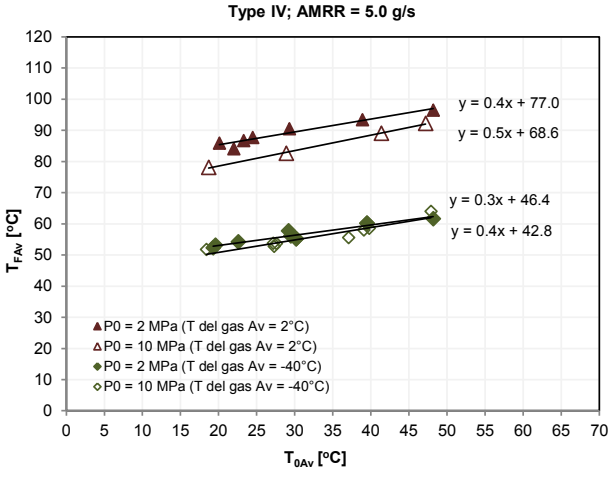

Fig. 8 – Gas temperatures reached at the end of the filling (TFAv) versus the initial temperature for fillings of Type IV tank for two different starting pressures (2 MPa and 10 MPa) and delivery temperatures of 2 °C and −40 °C.

CFD simulation results

In Fig. 9, the average gas temperature profiles in the adiabatic (a) and diathermal walls (b) refuelling simulations starting at 2 MPa pressure are shown. In Table 4, a summary of the average gas temperatures reached at the end of the filling (T_{FAv}) and the calculated State of Charge (SOC) at the end of the filling of the previously described simulations are shown. The linear regression of the T_{FAv} with the initial temperature (T_{0Av}) is also presented in Table 4.

Adiabatic simulations

Adiabatic calculations are instrumental in separating the effect of the heat transfer from the other phenomena that are involved in the process like gas compression and mixing of gas at different temperatures.

With adiabatic conditions and an initial pressure of 2 MPa, the final gas temperatures are very similar among each other for the three studied cases with less than 4 °C difference between them. Due to the small amount of gas that is inside the tank at the beginning of the filling, the effect of the initial temperature of the gas inside the vessel (i.e. −20 °C, 0 °C and 30 °C) on the final temperature is very limited. With an initial pressure of 2 MPa, the tank is almost empty at the beginning of the filling, containing only about 0.04–0.06 kg of hydrogen while the amount of gas that is injected into the tank is about 1 kg. The temperature at the end of the filling depends more on the temperature of the delivered gas than on the temperature of the gas initially in the vessel. That effect can be appreciated in first approximation from the Equation (3) which is derived from the conservation of energy for the mixing of ideal gases at different temperatures in adiabatic conditions, assuming constant heat capacity. T_{Mix} is the temperature of the gas mixture, T_{Av} and m_i are the temperature and mass of hydrogen inside the tank at the instant i and $T_{delgasAv}$ and m_{delgas} are the temperature and mass of the gas delivered at each instant i. Therefore, the increase of temperature is mainly due to the compression of the incoming gas and only in minor part due to the small amount of gas that is

Table 3 – Summary of the temperatures reached at the end of the filling and the SOC values observed for the maximum and minimum starting temperatures for different type IV and type III tanks, refuelled from 2 to 77 MPa at several AMRRs and fuel delivery temperatures.

				T_{FAv} (%)					
$T_{delgas\ Av}$ (°C)		20–25		2		−17		−40	
T_{0Av} (°C)		20	50	20	50	20	50	20	50
Type IV tank	3.7 g/s	96.0	111.6						
	5.0 g/s	99.7	111.1	85.92	97.32	69.2	81.8	52.4	63.2
Type III tank	3.3 g/s	76.5	94.2						
	6.5 g/s	83.4	100.8	70.60	88.0	59.5	75.1	44.6	61.4
				SOC (%)					
$T_{delgas\ Av}$ (°C)		20–25		2		−17		−40	
T_{0Av} (°C)		20	50	20	50	20	50	20	50
Type IV tank	3.7 g/s	89.6	87.0						
	5.0 g/s	89.0	87.1	91.4	89.4	94.6	92.2	98.0	95.8
Type III tank	3.3 g/s	93.2	90.0						
	6.5 g/s	91.9	88.8	94.3	91.1	96.5	93.5	99.7	96.1

initially in the tank. Moreover, for a constant initial pressure, the larger the initial temperature of the gas inside the tank, the smaller is the gas density and consequently smaller the amount of gas initially in the tank. With increasing the initial temperature of the gas inside the tank (and decreasing the amount of gas), the effect of the $T_{delgasAv}$ becomes even more dominant. Therefore, being constant $T_{delgasAv}$, the final temperature hardly changes with increasing T_{0Av} and the slope of the linear expression is small (0.07 in Table 4). Consequently and as it can be derived from Equation (2), the temperature of the gas in the tank (T_{0Av}) affects significantly the temperature increase ΔT_{Av} which decreases with increasing T_{0Av} from 149.5 °C (for the initial temperature of −20 °C) to 103 °C (for T_{0Av} of 30 °C). Injecting a gas at 0 °C in a colder gas at −20 °C ($T_{delgasAv} > T_{0Av}$) enhances the temperature increase due to compression while injecting a gas at 0 °C into a warmer gas at +30 °C ($T_{delgasAv} < T_{0Av}$) will mitigate the temperature increase (the latter effect is usually exploited in the pre-cooling procedure during the filling in refuelling stations to keep the final temperature below the 85 °C threshold). That explains the ΔT_{Av} decrease with increasing T_{0Av} (at constant $T_{delgasAv}$) with adiabatic walls. It must be emphasized that the above effect is caused by the gas mixing since the heat transfer is not included in the calculations.

$$T_{Mix} = \frac{T_{Av} m_i + T_{delgasAv}\, m_{delgas}}{m_i + m_{delgas}} \quad (3)$$

If a larger initial pressure is considered (~10 MPa), the difference in the final temperature is larger. For the 10 MPa adiabatic cases shown in Fig. 10, the difference for the three different initial temperatures considered is about 16 °C, four times larger compared to the 4 °C difference for the 2 MPa cases. With a larger initial pressure, the amount of gas initially inside the tank m_i is larger. Therefore, the effect of the initial gas temperature on the final gas temperature becomes more relevant. The slope of the linear expressions of T_{FAv} with T_{0Av} shown in Table 4 increased from 0.07 to 0.31 in the adiabatic cases when increasing from initial pressure of 2 MPa–10 MPa. That is consistent with a larger slope for the experimental data in Fig. 8 for the 10 MPa than for the 2 MPa initial pressures.

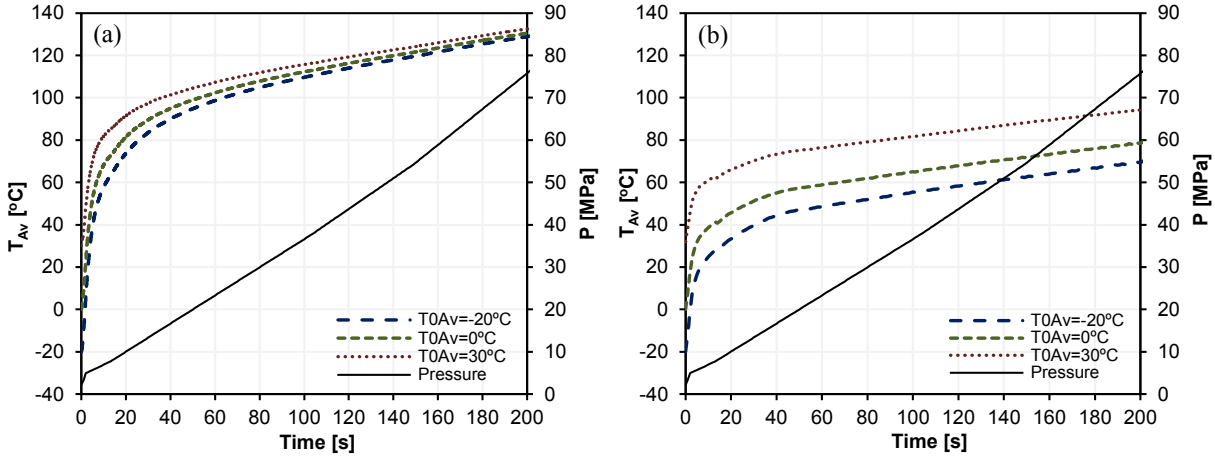

Fig. 9 – Average temperature profiles of the performed simulations for adiabatic (a) and diathermal walls (b); fillings of Type IV 29 L tank at initial tank temperatures of −20 °C, 0 °C and 30 °C and with a fuel delivery temperature of 0 °C.

Table 4 – The average gas temperatures reached at the end of the filling (T_{FAv}) and the State of Charge (SOC) for the refueling simulations (adiabatic and diathermal walls) of type IV tank with a fuel delivery temperature of 0 °C, an AMRR of 5.0 g/s, initial pressure of 2 MPa and 10 MPa and the three studied initial temperatures of −20 °C, 0 °C and 30 °C.

	T_{0Av} (°C)	−20	0	30	Lineal regression with T_{0Av}
P0 = 2 MPa	**Diathermal walls**				
	T_{FAv} (°C)	70.1	79.2	92.9	y = 0.45x + 79.5
	SOC (%)	93.4	91.7	88.9	
	Adiabatic				
	T_{FAv} (°C)	129.5	131.1	133.1	y = 0.07x + 131.0
	SOC (%)	83.3	83.1	82.8	
P0 = 10 MPa	**Diathermal walls**				
	T_{FAv} (°C)	60.6	71.5	87.7	y = 0.54x + 71.45
	SOC (%)	96.3	94.1	91.1	
	Adiabatic				
	T_{FAv} (°C)	102.6	109.5	118.4	y = 0.31x + 109.14
	SOC (%)	88.5	87.3	85.9	

Diathermal simulations

Since in the diathermal cases the heat transfer is taken into account in the CFD model, it is possible to identify the role of the heat transfer in the process by comparing the results from the adiabatic and the diathermal simulations. As shown in Table 4, the heat transfer in the diathermal walls results in lower final temperatures (70.1 °C–92.9 °C) than in the adiabatic cases (129.5 °C–133.1 °C). Moreover, the initial temperatures (mainly the wall temperature) affect the final gas temperatures more significantly in the diathermal cases (slope 0.45) than in the adiabatic cases (slope 0.1). This given example is for the 2 MPa initial pressure. For the 10 MPa initial pressure, the same effect has been also observed but in a lesser extent associated as explained before, to the bigger role played by the temperature of the gas inside the tank at the beginning of the filling.

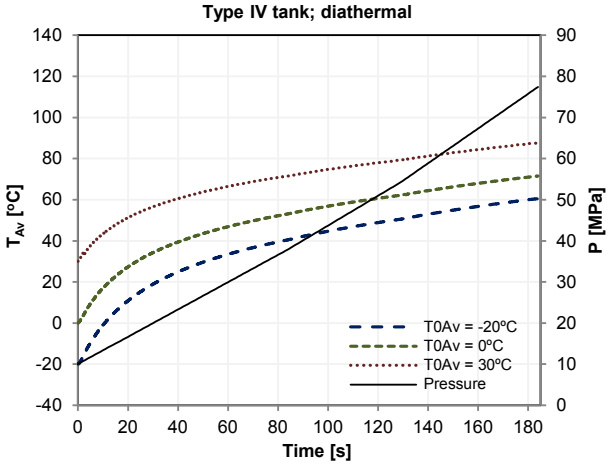

Fig. 10 – Temperature histories with adiabatic conditions, initial pressure 10 MPa, initial tank temperatures of −20 °C, 0 °C and 30 °C, and with a fuel delivery temperature of 0 °C.

As demonstrated for the adiabatic cases, $T_{delgasAv}$ has a more dominant effect on the final temperature compared to the initial gas temperature in the tank. In the diathermal cases, the temperature of the tank material plays a role due to the heat transfer. When $T_{delgasAv} > T_{0Av}$, the larger the difference between gas delivery temperature and the temperature of the tank material, the larger the heat transfer from the gas to the tank. On the contrary, when $T_{delgasAv} < T_{0Av}$, the larger the difference between the gas delivery temperature and the temperature of the tank material and thus, the smaller the heat transfer from the gas to the tank. Analysing the difference between diathermal and adiabatic cases (from the results shown in Table 4) it can be observed that the largest reduction of the maximum temperatures reached at the end of the filling when the heat transfer is included in the simulations occurs with −20 °C wall temperatures (59.4 °C when starting at 2 MPa and 42.0 °C when starting at 10 MPa). In that cases, the heat transfer from the gas to the tank material is larger compared to the cases with a higher wall temperature (0 °C and 30 °C), producing a larger mitigating effect on the temperature increase in the case with −20 °C than in the other cases (in the diathermal case compared to the adiabatic case). The effect on the final temperatures results also in a larger SOC increase for the −20 °C.

In principle the positive effect of a cold temperature in the tank walls on the gas temperature and the SOC could be exploited to contribute to keep the maximum gas temperature below the 85 °C threshold during refilling, reducing the required amount of pre-cooling. Using the vehicle air-conditioning system or another system to control the temperature of the tank compartment in extremely hot days is a strategy whose feasibility should be assessed in future investigations from the point of view of the technology, energy and cost issues.

Conclusions

Hydrogen refuelling experiments were carried out for type IV and type III tanks for different initial tank temperatures to investigate the effect of that parameter on the refuelling process. To better understand the occurring phenomena like gas compression, gas mixing and heat transfer, CFD simulations were performed with a validated model. The CFD results were consistent with the experimental findings. The results from adiabatic calculations were instrumental in separating the effects of the heat transfer from the effect of the gas mixing and compression.

With experimental data it was showed that the maximum gas temperature reached at the end of the filling increases linearly with the increase of the initial temperature while the temperature increase and the state of charge decreases linearly with increasing initial temperature. That behaviour was confirmed for different type of tanks, for different delivery gas temperatures and for different initial pressures inside the tank. In addition it was found that the slope of the linear expression for the final temperature is larger for the type III than for the type IV tank, and it increases with increasing initial pressure of the gas inside the vessel. It has been also observed that, on the contrary to what has been published in literature for hotter delivery temperatures, at high initial tank

temperatures (20 °C–50 °C) the increase of initial tank pressure does not result in an increase of the final temperature when the hydrogen is pre-cooled at −40 °C. This effect has been associated to the higher mass of colder gas injected in the tank when it is emptier which compensates the higher heat of compression when starting at lower pressure. This could be an advantage of using −40 °C pre-cooling in a hydrogen refuelling station.

In the adiabatic conditions and in an almost empty tank, the final temperature is weakly affected by the initial gas temperature. If the initial pressure is increased (and therefore the mass of gas that is initially inside the vessel) the influence of the initial gas temperature on the final temperature is also increased. The mixing of gas at different temperatures is the crucial phenomena for the effect of the initial gas temperature on the final temperature with adiabatic conditions.

Including the heat transfer in the calculations causes a reduction of the final temperature and an increase of the effect of the initial temperature (through the initial temperature of the tank material) on the final gas temperature. The colder the temperature of the tank walls, the larger the heat transfer, and the larger the temperature reduction compared to the adiabatic case.

The possibility to harness the mitigating effects of cold tank walls to reduce the use of pre-cooling during refilling will be the subject of future investigation by adopting methods to cool the tank when the ambient temperature is excessively high.

Acknowledgements

The authors acknowledge the GasTeF technicians F. Harskamp, K. Goblet and C. Bonato for the invaluable work in the preparation and execution of the experiments and M. Steen for his useful comments and remarks.

REFERENCES

[1] Corbo P, Migliardini F, Veneri O. Hydrogen as future energy carrier. In: Chapter 2 in hydrogen fuel cells for road vehicles. London: Springer; 2011. p.33–64.
[2] Maus S, Hapke J, Na Ranong C, Wuchner E, Friedlmeier G, Wenger D. Filling procedure for vehicles with compressed hydrogen tanks. Int J Hydrogen Energy 2008;33(17):4612–21.
[3] Barthélémy H. Hydrogen storage – recent improvements and industrial perspectives. In: International Conference of hydrogen energy; 2013. Brussel-Belgium.
[4] Fuel cells and hydrogen joint undertaking (FCH JU) Multi - Annual Work Plan 2014-2020, adopted by the FCH JU Governing Board on June 2014.
[5] Target Explanation Document: Onboard Hydrogen Storage for Light-Duty Fuel Cell Vehicles, U.S. DRIVE Partnership, revised on May 2015.
[6] GTR ECE/TRANS/WP.29/2013/41. Proposal for a global technical regulation (GTR) on hydrogen and fuel cell vehicles. June 2013.
[7] SAE J2579. Standard for fuel systems in fuel cell and other hydrogen vehicles. March 2013.
[8] Commission Regulation (EU) No 406/2010 of 26 April 2010. Implementing regulation (EC) No 79/2009 of the European parliament and of the council on type-approval of hydrogen-powered motor vehicles. May 2010.
[9] SAE J2601. Fueling protocols for light duty gaseous hydrogen surface vehicles. July 2014.
[10] Maus S. Modellierung und simulation der betankung von fahrzeugbehältern mit komprimiertem wasserstoff. Düsseldorf: Verlag; 2007 (879), Fortschr.-Ber., VDI Reihe 3VDI.
[11] Monde M, Kosaka M. Understanding of thermal characteristics of fueling hydrogen high pressure tanks and governing parameters. SAE Int J Alt Power 2013;2(1):61–7. http://dx.doi.org/10.4271/2013-01-0474.
[12] de Miguel N, Ortiz Cebolla R, Acosta B, Moretto P, Harskamp F, Bonato C. Compressed hydrogen tanks for on-board application: thermal behaviour during cycling. Int J Hydrogen Energy 2015;40(19):6449–58.
[13] de Miguel N, Acosta B, Moretto P, Ortiz Cebolla R. The effect of defueling rate on the temperature evolution of on-board hydrogen tanks. Int J Hydrogen Energy 2015;40(42):14768–74.
[14] Zhao L, Liu Y, Yang J, Zhao Y, Zheng J, Bie H, et al. Numerical simulation of temperature rise within hydrogen vehicle cylinder during refuelling. Int J Hydrogen Energy 2010;35(15):8092–100.
[15] Zheng J, Guo J, Yang J, Zhao Y, Zhao L, Pan X, et al. Experimental and numerical study on temperature rise within a 70 MPa type III cylinder during fast refuelling. Int J Hydrogen Energy 2013;38(25):10956–62.
[16] Acosta B, Moretto P, de Miguel N, Ortiz R, Harskamp F, Bonato C. JRC reference data from experiments of on-board hydrogen tanks refuelling. Int J Hydrogen Energy 2014;39(35):20531–7.
[17] Ortiz Cebolla R, Acosta B, Moretto P, Frischauf N, Harskamp F, Bonato C, et al. Hydrogen tank first filling experiments at the JRC-IET GasTeF facility. Int J Hydrogen Energy 2014;39(11):6261–7.
[18] Redlich O, Kwong JNS. On the thermodynamics of solutions: V. An equation of state: fugacity of gaseous solutions. Chem Rev 1949;44(1):233–44.
[19] de Miguel N, Acosta B, Moretto P, Ortiz Cebolla R. Influence of the gas injector configuration on the temperature evolution during refuelling of on-board hydrogen tanks. In: Hydrogen power theoretical and engineering solutions International Symposium; 2015. Toledo-Spain.
[20] Galassi MC, Papanikolaou E, Heitsch M, Baraldi D, Acosta Iborra B, Moretto P. Assesment of CFD models for hydrogen refuelling simulations. Int J Hydrogen Energy 2014;39(11):6252–60.
[21] Melideo D, Baraldi D, Galassi MC, Ortiz Cebolla R, Acosta Iborra B, Moretto P. CFD model performance benchmark of refuelling simulations. Int J Hydrogen Energy 2014;39(9):4389–95.
[22] ANSYS CFX. User's guide. Release 14.1. ANSYS Inc; 2013.
[23] Ouellette P, Hill PG. Turbulent transient gas injections. J Fluids Eng 2000;122(4):743–53.
[24] Pope SB. An explanation of the turbulent round-jet/plane-jet abnormality. Tech Note AIAA 1978;16(3):279–81.
[25] Magi V, Iyer V, Abraham J. The k-e model and computed spreading in round and plane jets. Numer Heat Transf 2001;40:317–34.
[26] NIST chemistry webbook. Available via the internet at: http://webbook.nist.gov/chemistry.
[27] de Miguel N, Acosta B, Baraldi D, Melideo D, Ortiz Cebolla R, Moretto P. Experimental and numerical analysis of refueling of on-board hydrogen tanks at different ambient temperatures. In: World hydrogen energy conference; 2014. Gwangju-Korea.
[28] Kim SC, Lee SH, Yoon KB. Thermal characteristics during hydrogen fueling process of type IV cylinder. Int J Hydrogen Energy 2010;35(13):6830–5.
[29] Ortiz Cebolla R, Acosta B, Moretto P, de Miguel Echevarria N. Effect of precooled inlet gas and mass flow rate on final state of charge during hydrogen refuelling. Int J Hydrogen Energy 2015;40(13):4698–706.